Mixed Polyelectrolyte−Surfactant Langmuir Monolayers at the Air/Water Interface

Yuh-Lang Lee,* Anna Dudek, Tai-Nian Ke, Fang-Wei Hsiao, and Chien-Hsiang Chang

Department of Chemical Engineering, National Cheng Kung University, Tainan 70101, Taiwan

Received April 17, 2008; Revised Manuscript Received June 10, 2008

ABSTRACT: Polystyrenesulfonate acid (PSS) and alkyltrimethylammonium bromide (C_nTAB, n = 8, 14, or 18) were dissolved in a chloroform/methanol solution and cospread on an air/water interface. The surfactant−polyelectrolyte interaction leads to the formation of hydrophobic complexes which are able to spread well at the air/water interface. The effects of surfactant chain length and surfactant/polymer ratio on the characteristics of the mixed monolayers were studied in terms of surface pressure−area (π−A) isotherm, area relaxation, and hysteresis behavior as well as the surface morphology and composition of the corresponding Langmuir−Blodgett films. The mixed monolayers prepared by cospreading method are also compared with the complex monolayers prepared by preprecipitation of the surfactant−polyelectrolyte complexes from an aqueous solution. The experimental results show that the chain length of an incorporated surfactant is the main factor determining the properties of a complex monolayer. By using a longer chain surfactant to complex with polyelectrolyte, a more condensed monolayer with higher collapse pressure and stability can be obtained. For the effect of surfactant/polymer ratio (S/P), it is found that an increase of S/P ratio not only produces more complexes capable of staying at the air/water interface but also affects the incorporation of uncomplexed surfactant into the mixed monolayer. The X-ray photoelectron spectroscopy (XPS) analysis shows that the amount of uncomplexed surfactant is higher at low S/P value (0.2) and is insignificant when the S/P value increases to about 1.0 or 2.0, where a maximum amount of complexes were formed at the interface. A further increase of S/P ratio may cause additional incorporation of uncomplexed surfactant and/or micellization of surfactant around PSS cores, depending on the surfactant chain length. A model illustrating the incorporation and spreading of the surfactant−polyelectrolyte complexes at the air/water interface was proposed.

Introduction

Langmuir monolayers at the air/water interface have attracted broad interest not only to study the two-dimensional interaction between molecules but also for preparing molecular thin films with controllable structure and morphology. A majority of studies on Langmuir monolayers and their corresponding Langmuir−Blodgett (LB) films were performed on small molecules with amphiphilic properties. For the high-molecular-weight polymers which possess unique properties like thermal, mechanical, and chemical stability, only minor attention was paid to monolayer studies.[1–5]

Polyelectrolytes are an interesting class of polymers because of the charge distributed along the main or side chains of the molecule. The charge leads not only to attractive electrostatic interactions with oppositely charged compounds but also to repulsive electrostatic interactions between monomer units, causing an expanded structure of a polymer chain.[6,7] Polyelectrolytes and ionic surfactants of opposite charge have strong interactions, caused by the electrostatics, leading to a synergistic effect that is often used in industrial applications to enhance properties such as surface adsorption and bulk rheology.[8–23] The polyelectrolyte−surfactant interaction was also known to allow formation of hydrophobic complexes both in the bulk and at the air/water interface. By using the electromotive force measurement, Monteux et al. studied the polyelectrolyte−surfactant interaction in bulk solution.[12–14] Their results showed that, with increasing surfactant concentration, the polymer−surfactant interaction first occurs in the bulk and then, just before bulk precipitation of complexes, the surfactant−polymer complexes adsorb at the air/water interface forming an interfacial gel. The structures of the adsorbed layers of the polymer−surfactant mixtures were reported to depend on the surfactant concentration, surfactant chain length, and surfactant/polymer ratio.[12–14,24–26]

For polyelectrolytes which possess high water solubility, it is difficult to study their Langmuir monolayer behavior. To make this study possible, the polyelectrolyte should be hydrophobized (by alkylation) to increase stability at the air/water interface. However, only few studies were found which dealt with the direct spreading of a hydrophobized polyelectrolyte at the air/water interface.[6,27–29]

Inspired by the strong polyelectrolyte−surfactant interaction in a bulk aqueous solution, we demonstrate a method to form polyelectrolyte−surfactant complexes directly on the water surface to study the Langmuir monolayer behavior of these complexes. Polystyrenesulfonate acid (PSS) and a cationic surfactant (alkyltrimethylammonium bromide, C_nTAB, n = 8, 14, or 18) are dissolved together in an appropriate solvent to prevent the precipitation of the complexes. The mixture was spread directly on the water surface where the hydrophobized complexes form an extended Langmuir monolayer. The effects of the surfactant chain length and surfactant/polymer ratio on the behavior and property of the Langmuir monolayers are studied in the present work. In an alternative approach, the surfactant−polymer complexes are preprecipitated from an aqueous solution and used to prepare a Langmuir monolayer. The mixed surfactant−polymer monolayers prepared by cospreading method and by preprecipitation of the complexes are compared in terms of surface pressure−area (π−A) isotherm, area relaxation, hysteresis behavior, and morphology of corresponding LB films observed by atomic force microscopy (AFM).

Experimental Section

Materials. Sodium polystyrenesulfonate (SPSS, M_w = 70 000) and polystyrenesulfonate acid (PSS, M_w = 75 000) were purchased from Aldrich. Octyltrimethylammonium bromide (C_8TAB), tet-

* Corresponding author: Tel 886-6-2757575ext 62693; Fax 886-6-2344496; e-mail yllee@mail.ncku.edu.tw.

10.1021/ma800855h CCC: $40.75
Published on Web 07/12/2008

radecyltrimethylammonium bromide (C_{14}TAB), and octadecyltrimethylammonium bromide (C_{18}TAB) were supplied by Fluka, Sigma, and Aldrich, respectively. Doubly distilled water purified with a Milli-Q apparatus supplied by Millipore (resistivity ≥ 18 MΩ·cm) was used in all the experiments of this study.

Mixed PSS/C_nTAB Monolayer and LB Film Preparation. In the present study, mixed C_nTAB-PSS ($n = 8$, 14, or 18) monolayers were prepared by two approaches. For the first one (method 1), PSS and surfactant were mixed and dissolved in a chloroform/methanol (7:3 by volume) solution. The concentration of PSS in the solution was kept at 0.5 mg/mL, and various amounts of C_nTAB were added to control the ratio of PSS-to-surfactant. For method 2, SPSS and C_nTAB ($n = 14$ or 18) were individually dissolved in water first, followed by mixing the two solutions. The interaction between SPSS and C_nTAB produces a complex with poor water solubility which precipitates in the aqueous solution. The precipitate was repeatedly washed by water for about 20 times and then dried in a vacuum dryer at room temperature. Finally, the dried product was dissolved in chloroform to prepare a stock solution with a concentration of 0.5 mg/mL based on the PSS and used for monolayer study.

Elemental analysis was used to measure the molar ratio of surfactant molecules associated with the SPSS repeat unit (CTAB/SPSS) in the precipitate. The experiment was performed using a commercial elemental analyzer (Elemental Vario EL III). From this analysis, the C/N atomic ratio can be obtained for the C_nTA−PSS complex. Since there is only one N atom in a surfactant molecule and only one S atom in a monomer unit of PSS, the (C_nTAB/SPSS) ratio is equivalent to the N/S atomic ratio. The relation between atomic ratios of N/S and C/N depends on the carbon atoms contained in a surfactant (n) according to the following equation:

$$(C_nTAB/SPSS) = N/S = 8/(C/N - n) \quad (1)$$

where 8 is the number of carbon atoms per SPSS repeat unit.

A Langmuir film balance (KSV2000, KSV Instruments Ltd., Finland) with a working area of 75×515 mm^2 was used to conduct the monolayer experiments. The film surface pressure at the air/water interface was measured by using the Wilhelmy plate arrangement attached to a microbalance. After spreading an appropriate amount of stock solution on the air/liquid interface, a waiting period of 20 min was allowed for solvent evaporation. The monolayer was then compressed at a rate of 5 mm/min. A surface pressure−area (π−A) isotherm was obtained by continuous compression of the monolayer using two moving barriers. All the experiments were performed at constant temperature of 25 °C.

To prepare LB films of the mixed surfactant−PSS monolayers, freshly cleaved mica plates (Alfa Aesar) were used as substrates. The substrate was immersed into the subphase before the spreading of the monolayer. After the monolayer was compressed to the target surface pressure, the monolayer was transferred at a rate of 1 mm/min in the upward stroke and one layer of a LB film was prepared. During the deposition, the surface pressure was kept constant by adjusting the barriers automatically. The LB films were dried in a desiccator at room temperature for about 5 days.

The morphology of the LB films was examined with an AFM (Digital Instrument, Nano Scope III a) via tapping mode at a scan rate of 0.5 Hz. A silicon tip on a cantilever of 125 μm length (noncontact silicon cantilever, model NCH-50, Germany) was used. The resonance frequency and force constant of the tip are 320 kHz and 42 N/m, respectively. The chemical elements of the LB films were analyzed by a X-ray photoelectron spectroscopy (XPS) equipped with a Mg Kα source (1253.6 eV) (ESCA 210, VG Scientific Ltd.).

For the various analysis methods performed in this work, experiments were repeated to check their reproducibility. The reproducibility is found to be good enough to distinguish the different properties of the monolayers prepared at various conditions.

Results and Discussion

Surface Pressure−Area per Molecule (π−A) Isotherm. The monolayer behaviors of polystyrenesulfonate acid (PSS) and surfactants C_nTAB were first examined individually. By spreading only PSS or only C_nTAB ($n = 8$, 14, or 18) on the air/water interface, no significant elevation of the surface pressure can be detected during compression. This result indicates that the solubility of these compounds in water is too high to form a stable Langmuir monolayer at the air/water interface.

When a mixed C_nTAB−PSS stock solution was spread on the water surface, a stable monolayer can be formed as revealed by the significant pressure elevation during the compression. Apparently, the interaction of PSS and C_nTAB leads to a polymer−surfactant complex which is able to remain at the air/water interface. The π−A isotherms of the mixed C_nTAB−PSS monolayers are shown in Figure 1, which demonstrate a strong dependence of isotherms on the C_nTAB/PSS ratio and on the chain length (i.e., the n value) of a surfactant.

For the mixed C_8TAB−PSS monolayers shown in Figure 1a, the π−A isotherm shifts right steadily with increasing C_8TAB/PSS ratio. It is noteworthy that the area per repeat unit (A) for an isotherm is calculated based on the total repeat units of PSS spread on the subphase, which is not anticipated to be present completely at the air/water interface. Therefore, a right shift of the isotherm with increasing amount of surfactant addition indicates that more C_8TAB−PSS complexes exist at the air/water interface since more surfactant molecules are available to form the complex. The surfactant−PSS interaction may occur in the spreading solvent and/or at the interface after spreading. It is inferred that the electrostatic force between oppositely charged surfactant and polymer is the major interaction in forming the surfactant−PSS complexes. However, van der Waals (VDW) and polar interactions will also contribute to the incorporation of the two components.

All the isotherms of the mixed monolayers exhibit steeper curves in a region between $\pi = 5$ and 15 mN/m, and their slopes become smaller after encountering a phase transition point. The phase transition point here is considered as the collapse point of a mixed monolayer, and the surface pressure corresponding to this point indicates the highest pressure that the monolayer can sustain before the collapse of a monolayer. The collapse pressures for the mixed C_8TAB−PSS monolayers are low in general, with similar values ranging between 15 and 16 mN/m, attributable to the short alkyl chain contained in a C_8TAB molecule. The similar features (including collapse pressure and slope of the curves) for isotherms obtained at various C_8TAB/PSS ratios imply similar properties of these monolayers, which also sustains the inference that the right shift of an isotherm is mainly caused by the increase of complex molecules presented at the interface.

The isotherms of the mixed monolayers approach the right-most state at a C_8TAB/PSS ratio of 2.0, and further increase of the C_8TAB/PSS ratio does not cause a significant shift to the isotherm. The monolayer corresponding to the right-most shift of the isotherm is supposed to be in a state that nearly all the PSS molecules spread on the subphase were associated with the C_8TAB, forming stable complexes and remaining at the interface. The C_8TAB/PSS ratio (2.0) required to approach this state indicates that a higher amount of C_8TAB is necessary for all the PSS molecules to interact with C_8TAB, either in the spreading solvent or at the interface. At the present stage, it is not clear whether all the repeat units of PSS are associated with C_8TAB in 1:1 ratio. It is inferred that the hydrophobicity (the chain length) of the incorporated surfactant will affect the minimum incorporation ratio of surfactant-to-PSS units for

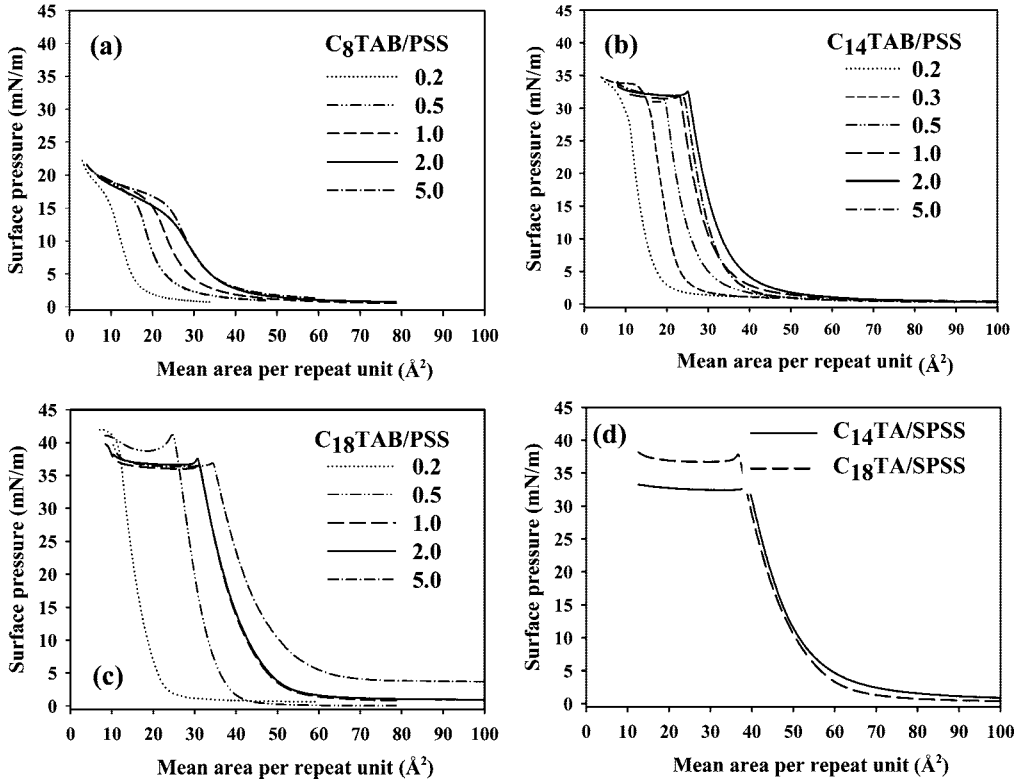

Figure 1. $\pi-A$ isotherms of mixed C_8TAB−PSS (a), C_{14}TAB−PSS (b), and C_{18}TAB−PSS (c) monolayers with various C_nTAB/PSS ratios prepared by cospreading. The $\pi-A$ isotherms of C_{14}TA−PSS and C_{18}TA−PSS complex monolayers prepared by preprecipitation are shown in (d).

forming a stable complex molecule. The incorporation ratio of surfactant-to-PSS units will be analyzed by XPS and discussed later.

The isotherms of mixed C_{14}TAB−PSS and C_{18}TAB−PSS monolayers, shown in Figures 1b,c, demonstrate a different feature compared with that of the C_8TAB−PSS monolayers. By using the surfactants with longer chain lengths, the isotherms become steeper, indicating the formation of more condensed monolayers. Moreover, the collapse pressure of the mixed monolayer increases to about 33 ± 1 mN/m for C_{14}TAB−PSS and to about 39 ± 2 mN/m for C_{18}TAB−PSS. Apparently, the incorporation of a more hydrophobic surfactant to the polyelectrolyte leads to a mixed monolayer that can sustain a higher surface pressure before collapse. The effect of C_{14}TAB/PSS or C_{18}TAB/PSS ratio on the shift of the isotherms has a similar tendency as that for the mixed C_8TAB−PSS monolayer. However, the right-most shift of the isotherm for the two longer surfactants was approached at a smaller surfactant/PSS ratio (∼1.0), compared with the ratio for C_8TAB−PSS (∼2.0), indicating a more efficient incorporation of a longer surfactant to the PSS. For the mixed C_{18}TAB−PSS monolayer, the isotherm can further extend, after adsorption of the maximum amount of complexes, when a higher excess amount of C_{18}TAB was presented (C_{18}TAB/PSS = 5). This phenomenon is inferred to be the presence of more C_{18}TAB at the air/water interface due to its relatively higher hydrophobicity. This inference was sustained by the XPS analysis which shows that the C_{18}TAB

Table 1. Monolayer Properties Taken from the Isotherms of the Mixed C_nTAB−PSS Monolayers

surfactant chain length	C_nTAB/PSS ratio	collapse pressure (mN/m)	$(\partial\pi/\partial A)$ at $\pi = 10$ (for C_8) $\pi = 25$ (C_{14}, C_{18})	N/S ratio in the LB film[a]	rms roughness of the LB films (nm)
C_8	0.2	16.0	−2.2881	1.78	0.26
	0.5	15.6	−1.9586		
	1.0	15.0	−1.4785		
	2.0	13.5	−1.1098	1.03	0.31
	5.0	15.0	−1.3575	1.07	0.24
C_{14}	0.2	34.0	−6.2813	1.67	0.11
	0.3	34.0	−4.8723		
	0.5	32.0	−4.4250		
	1.0	32.0	−4.4156	0.90	0.13
	2.0	33.0	−3.5375		
	5.0	32.0	−4.0875	1.11	0.16
C_{18}	0.2	42.0	−4.9524	1.86	0.10
	0.5	42.0	−4.7547		
	1.0	37.0	−2.7160	0.91	0.08
	2.0	38.0	−2.9737		
	5.0	37.0	−2.1681	1.29	0.90
C_{14}TA−PSS		33.0	−2.5000	1.03[b]	0.20
C_{18}TA−PSS		38.0	−2.6234	0.90[b]	0.20

[a] N/S ratio analyzed by XPS corresponds to the molar ratio of surfactant-to-monomer units of polyelectrolyte in the mixed monolayer. [b] Data obtained from elemental analysis of the preprecipitated complexes.

has a higher surface composition in comparison with PSS units (N/S = 1.29) in the corresponding LB film (shown in Table 1).

For the three systems shown above, it is interesting to find that the collapse pressure of the mixed monolayer is higher at low surfactant/PSS ratio (0.2) and decreases slightly with increasing concentration of surfactant (Table 1). The different collapse pressures, as well as the slight difference in the slopes of the isotherms, imply different properties (chain configuration and/or composition) of the mixed monolayers prepared at various surfactant/PSS ratios.

Figure 1d shows the $\pi-A$ isotherms of monolayers for C_nTA−PSS complexes prepared by preprecipitation of SPSS with C_nTAB (n = 14, 18). It is noteworthy that the C_8TA−PSS precipitate cannot be collected due to its high solubility in water; therefore, C_8TA−PSS monolayer was not studied by this method. According to the result shown in Figure 1d, there is no significant difference between isotherms of the two mixed monolayers except for the collapse pressure. The collapse pressures measured for the two mixed monolayers are 33 and 38 mN/m respectively for C_{14}TA−PSS and C_{18}TA−PSS. Because the C_nTA−PSS complexes were formed by preprecipitation in water, the two complexes should have similar hydrophobicity. Elemental analysis was performed to measure the ratio of surfactant molecules complexed to the repeat units of PSS (C_nTA/PSS). The N/S ratios measured for the C_{14}TA−PSS and C_{18}TA−PSS complexes are 1.01 and 0.90, respectively, indicating that C_{14}TAB molecules were incorporated to the repeat unit of PSS in nearly 1:1 ratio, but a lower ratio of C_{18}TAB was required to form a complex of similar hydrophobicity. The nearly identical isotherms for the two mixed monolayers indicate the similar configuration and extensibility of the two complexes at the air/water interface. However, the complex hydrophobized by a longer surfactant (C_{18}TA−PSS) can sustain a higher pressure before collapse of the monolayer.

Comparing the isotherms of the C_nTAB−PSS (n = 14 or 18) monolayers prepared by the cospreading (at the right-most shift state) and preprecipitation methods, the collapse pressures are nearly identical for the same polymer−surfactant system. However, the mean limiting molecular area for the mixed monolayer prepared by preprecipitation is higher than the area prepared by cospreading of the same polymer−surfactant system. These results imply that the mixed monolayers prepared by the two approaches have similar properties, but the mixed monolayer prepared by preprecipitation seems to exist in a higher amount or/and in a more extended form at the interface. The states of monolayers can also be compared by the Gibbs elastic modulus, E, which is defined as the reciprocal of monolayer compressibility, C.

$$E = 1/C = -A(\partial\pi/\partial A) \quad (2)$$

Although the precise molecular area can not be obtained for the cospreading monolayers, the slopes of $\pi-A$ curves, $\partial\pi/\partial A$, can also be used to evaluate the elastic moduli of the monolayers. The slopes of the $\pi-A$ isotherms are measured and listed in Table 1 which show that monolayers prepared by preprecipitation method have nearly identical slopes, indicating similar configurations and extensibility of the monolayers prepared by this method. On the contrary, the slopes measured for the cospreading C_{14}TAB−PSS and C_{18}TAB−PSS monolayers, shown in Figures 1b,c, are not identical. Furthermore, the slopes of the cospreading monolayers are different from the monolayers prepared by preprecipitation. These results indicate not only the different properties between C_{14}TAB−PSS and C_{18}TAB−PSS mixed monolayers but also the distinct behaviors of the mixed monolayers prepared by the two approaches. The smaller slopes measured for the monolayers prepared by preprecipitation suggest that these monolayers are present is a more expanded state, compared with monolayers prepared by cospreading method.

For the adsorption of mixed polyelectrolyte−surfactant monolayer from an aqueous solution, few papers studied the compression behavior of the adsorbed monolayer. A typical case was made by Jain et al. using an anionic polyelectrolyte (polyacrylamide sulfonate, PAMPS) and a cationic surfactant (cetyltrimethylammonium bromide).[30,31] Compared with the Langmuir monolayer in the present study, the adsorption monolayer revealed a more expanded state, higher compressibility, and lower phase transition pressure during surface compression. Furthermore, the $\pi-A$ isotherms are strongly dependent on the surfactant concentration. An increase of the surfactant concentration always leads to a significant decrease of surface pressure of the monolayers. Apparently, the compression characteristics of the adsorption monolayers are highly different from those of the Langmuir monolayer prepared by the spreading method, which also implies different properties of the monolayers prepared by the two methods.

Area Relaxation of the Mixed Monolayer. In a series of experiments concerning area relaxation phenomena (Figure 2), it was found that the kinetic stability of mixed C_nTAB−PSS monolayer depends on the surfactant chain length and the surfactant/polymer ratio. For C_8TAB−PSS (Figure 2a), the A/A_0 value after 60 min relaxation was 0.9 at C_8TAB/PSS ratio of 0.2. With an increase of C_8TAB/PSS ratio, the A/A_0 value increases, indicating that the mixed monolayer becomes more stable. When a surfactant with a longer chain length was used, the monolayer stability increases as evaluated by the higher A/A_0 value after relaxation. However, a contrary effect of surfactant/polymer ratio on the monolayer stability was observed. For the C_{14}TAB−PSS (Figure 2b), the A/A_0 value after 60 min relaxation was 0.97 at low C_{14}TAB/PSS ratio (0.2 and 0.3) and decreases to about 0.93 at high C_{14}TAB/PSS ratios. The mixed C_{18}TAB−PSS monolayers have the highest relaxation stability (Figure 2c) among the three studied systems. After relaxation, the A/A_0 value is higher than 0.97 and is nearly independent of the surfactant/polymer ratio. For the monolayers prepared by preprecipitation of complexes (Figure 2d), the A/A_0 values after 60 min relaxation are 0.95 and 0.98 respectively for C_{14}TA−PSS and C_{18}TA−PSS.

The results of monolayer relaxation studies obtained for the preprecipitated complexes clearly indicate that the complexes formed by a longer surfactant have better stability, which also implies that the area loss in the relaxation is due to the dissolution of complexes into the subphase. For the monolayers prepared by cospreading, the effect of surfactant chain length on the relaxation stability also sustains the above inference. However, the surfactant/polymer ratio dependence of the relaxation stability reveals the different composition of mixed monolayers prepared at various ratios. The contrary effect of surfactant/polymer ratio on the relaxation stability between C_8TAB−PSS and C_{14}TAB−PSS was attributed to the ability of a surfactant that can stably stay at the air/water interface. As will be shown later, the ratios of surfactant-to-PSS units on the monolayers of the three systems were measured to be about 1.7 and 0.9−1.0 respectively for surfactant/polymer ratios of 0.2 and 1.0 (Table 1). That is, a large excess amount of surfactant molecules is present simultaneously with the complexes at low surfactant/polymer ratio (0.2). For the C_8TAB that has low hydrophobicity, the uncomplexed surfactant is easy to dissolve into water during the relaxation process. Therefore, the monolayer containing more uncomplexed surfactant (at surfactant/polymer ratio = 0.2) has a higher area loss compared to the monolayer with less uncomplexed surfactant (high surfactant/polymer ratio). For the C_{14}TAB that has higher hydrophobicity, the uncomplexed surfactant plays an additional

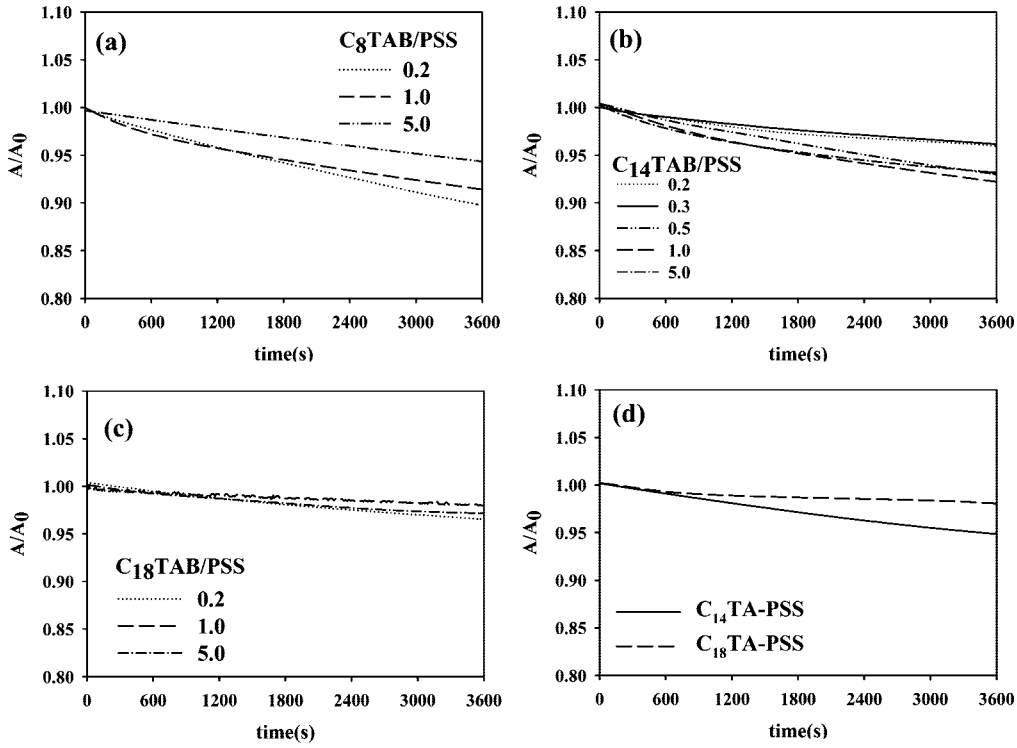

Figure 2. Area−relaxation behavior of mixed C_8TAB−PSS (a), C_{14}TAB−PSS (b), and C_{18}TAB−PSS (c) monolayers with various C_nTAB/PSS ratios prepared by cospreading. The relaxation curves of C_{14}TA−PSS and C_{18}TA−PSS complex monolayers prepared by preprecipitation are shown in (d).

role to enhance the stability of the complexes probably due to the VDW and/or polar interaction. Therefore, a contrary effect of surfactant/polymer ratio was obtained.

Hysteresis Behavior. Three consecutive compression−expansion cycles were preformed on the mixed monolayers to evaluate their respreading characteristics after compression. Figure 3a shows the hysteresis curves of a mixed C_8TAB−PSS monolayer. Because the hysteresis behaviors for various surfactant/polymer ratios are similar, only the result at molar ratio 1.0 is shown as a representative. For each cycle shown in Figure 3a, the expansion curve closely follows the compression route, indicating insignificant hysteresis and the high respreading characteristic of this monolayer. However, the compression−expansion loops left shift cycle by cycle, attributing to the loss of the monolayer by dissolution into the subphase. This result is consistent with the higher area loss of C_8TAB−PSS monolayer measured in the relaxation experiments. Both are ascribed to the comparatively higher solubility of C_8TAB in water.

The hysteresis behavior of mixed C_{14}TAB−PSS and C_{18}TAB−PSS monolayers are similar; therefore, only the results of mixed C_{14}TAB−PSS monolayer are shown (in Figures 3b,c) as representatives. At a small C_{14}TAB/PSS ratio of 0.2 (Figure 3b), the expansion curve of the first cycle is shifted left in comparison with compression, indicating the compressed monolayer cannot recover to a state before compression. However, no significant hysteresis was observed for the following compression−expansion cycles. The compression and expansion curves of the second and third cycles overlap almost completely, following closely the expansion route of the first cycle. When the C_{14}TAB/PSS ratio was increased to 1.0 or 5.0, the hysteresis between compression and expansion processes does not appear in all the cycles (Figure 3c). The identical curves for various loops indicate that a respreadable and stable monolayer was formed at the spreading stage. The monolayer hysteresis in the first compression−expansion cycle for monolayer prepared at C_{14}TAB/PSS = 0.2 is inferred to be a result of surfactant loss under compression. Because this monolayer was measured to be surfactant-rich, it is possible that the uncomplexed surfactant will be forced into subphase in the first compression stage, leading to a left shift of the expansion curve. For the monolayer with fewer uncomplexed surfactant (C_{14}TAB/PSS = 1.0), this effect does not occur, and therefore, no hysteresis was observed.

The hysteresis behavior of the complex monolayers prepared by preprecipitation is shown in parts a and b of Figure 4 for C_{14}TA−PSS and C_{18}TA−PSS, respectively. In each cycle, identical curves were obtained for compression and expansion stages. However, the hysteresis loop slightly left shifts cycle by cycle. This phenomenon is especially obvious for the complex with shorter surfactant, C_{14}TA−PSS. Therefore, the left shift of the hysteresis loop was inferred to be the dissolution of complexes with low hydrophobicity. Although the precipitate was repeatedly washed by water to remove the complexes of low hydrophobicity, a complex that can sustain the water washing in bulk solution does not need to stay stably on the water surface because a complex was supposed to be present in a highly extended state at the air/water interface. It is interesting to find that the hysteresis behavior of the monolayers prepared by the preprecipitation approach are different from the corresponding systems prepared by the cospreading method, implying different structures between monolayers prepared by these two methods.

Surface Morphology and Composition of the Mixed Monolayer. Mica was used as substrates to deposit one layer of the monolayer by the LB deposition technique. The transfer ratio measured during the upstroke deposition was close to unity for each system studied here. Figure 5 shows the AFM images of mixed C_8TAB−PSS monolayers transferred at $\pi = 10$ mN/m with C_8TAB/PSS ratios of 0.2, 2.0, and 5.0. Figure 5 shows that the C_8TAB−PSS LB films have a loosely packed morphology, consisting of dark holes distributed among the films. The film thickness measured from the depths of holes ranges between 0.7 and 0.9 nm, indicating the well-extended status of the mixed

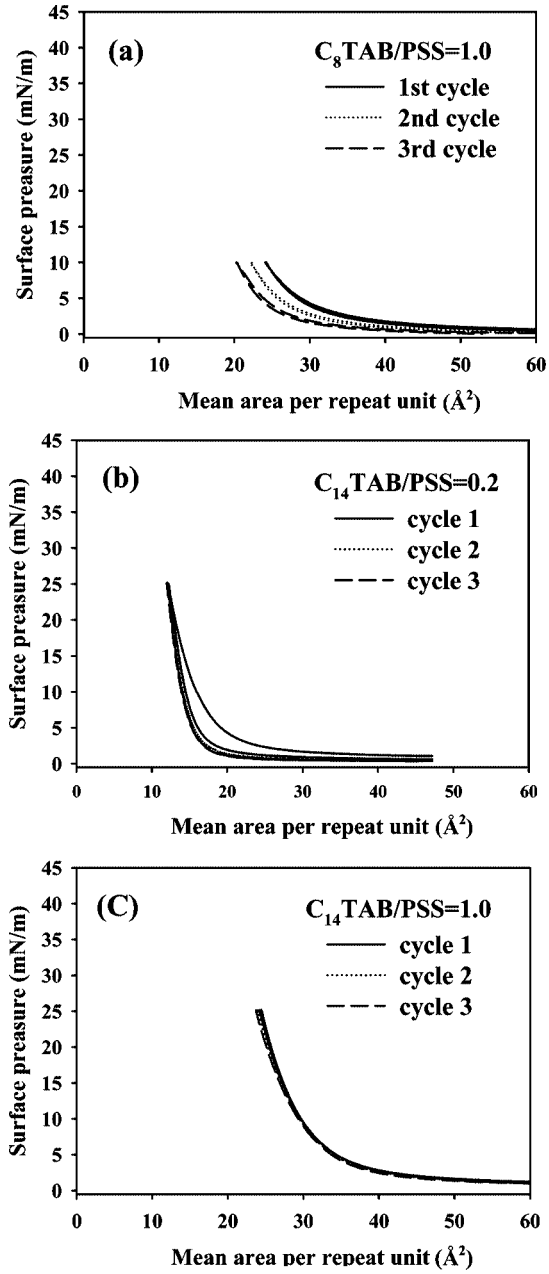

Figure 3. Hysteresis curves of mixed C_8TAB−PSS monolayer prepared by cospreading at C_8TAB/PSS 1.0 (a) and C_{14}TAB−PSS monolayer at C_{14}TAB/PSS ratios of 0.2 (b) and 1.0 (c).

monolayers without significant aggregative structure. Figure 5 also shows that variation of the ratio causes little change to the film morphology. When a surfactant with a longer chain length was used instead, smoother film morphologies were obtained as shown in Figures 6 and 7 for C_{14}TAB−PSS and C_{18}TAB−PSS mixed monolayers, respectively. The holes present on the C_8TAB−PSS film do not appear on the two systems, indicting the formation of a more condensed monolayer. For identifying the difference in surface morphologies of these smoother films, a different scale bar (3 nm) was used for the two systems, and the root-mean-square (rms) roughness values measured for the various films are listed in Table 1. For the C_{14}TAB−PSS films, an increase of the C_{14}TAB/PSS ratio results in a slightly rougher morphology. The rms roughness increases from 0.11 to 0.16 nm as the ratio increases from 0.2 to 5.0.

For the C_{18}TAB−PSS films, a more even morphology was imaged for C_{18}TAB/PSS ratios of 0.2 and 1.0. However, obvious

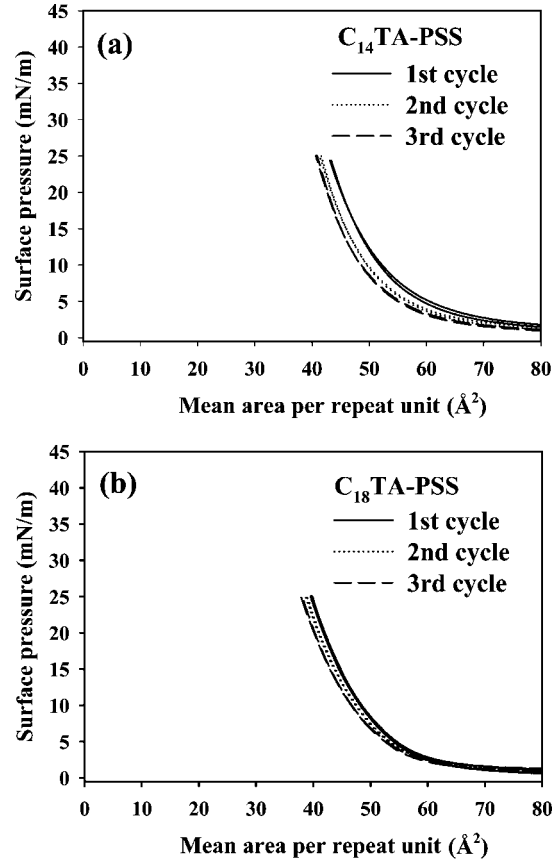

Figure 4. Hysteresis curves of the complex monolayers of C_{14}TA−PSS (a) and C_{18}TA−PSS (b) prepared by preprecipitation.

aggregates, with a height of about 3.8 nm, appeared when the ratio increases to 5.0. The formation of the aggregates seems to associate with the further right shift of the isotherm of the C_{18}TAB−PSS monolayer shown in Figure 1c. Apparently, the higher hydrophobicity of C_{18}TAB triggers a higher incorporated amount of the surfactant into the mixed monolayer. Because the height of the aggregates (about 3.8 nm) is ∼2 times the molecular length of C_{18}TAB, these aggregates are inferred to be surfactant micelles with bilayer structure. According to the previous studies on polyelectrolyte−surfactant interactions in aqueous solution, surfactant may micellize or aggregate around a polymer core at surfactant concentrations below critical micelle concentration (cmc).[12–14,32–35] Interfacial microgels or micelles form as a result and adsorb to the air/liquid interface in association with the polymer−surfactant complexes. For the present case, although little amount of surfactant is spread on the water surface, it is possible that local surfactant concentration around the interface may attain a value high enough for micellization. According to this mechanism, a larger amount of excess surfactant is present in the complex monolayer, which is responsible for the further right shift of isotherm as well as a higher N/S ratio (1.29) of the corresponding monolayer. However, this effect is likely to occur only in C_{18}TAB−PSS, at elevated C_{18}TAB concentrations, because a surfactant with longer chain length micellizes at a lower concentration than a shorter surfactant.

The AFM images of the complex monolayers prepared by preprecipitation method are shown in Figure 8. Although the isotherms for C_{14}TA−PSS and C_{18}TA−PSS monolayers are quite similar, the film morphologies corresponding to the two films are not completely identical. A well-expanded film comprising small holes is observed on the C_{14}TA−PSS film. However, on the C_{18}TA−PSS film, the hole density decreases and the film tends to have a more continuous morphology. The

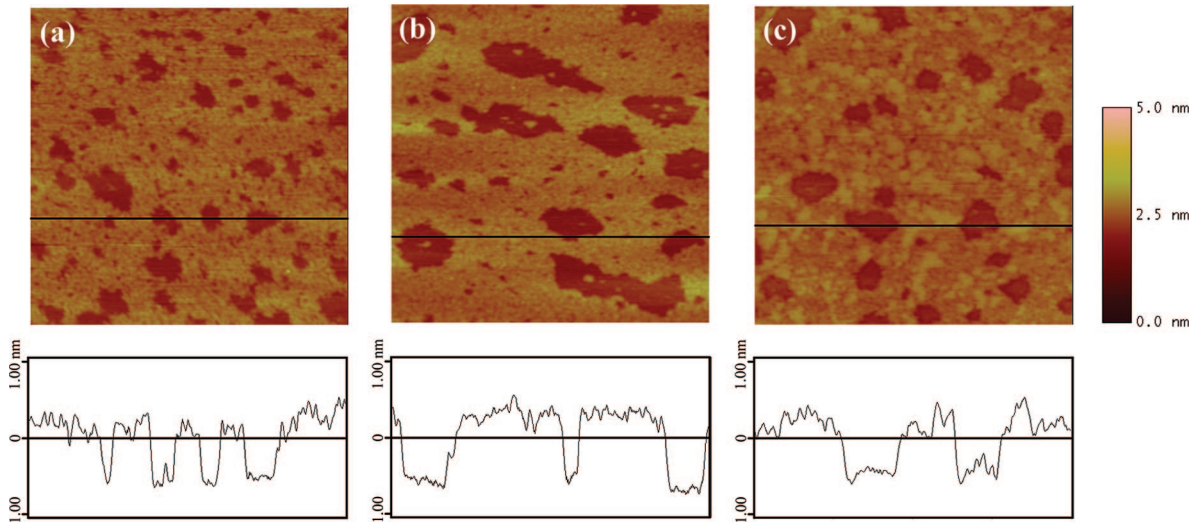

Figure 5. AFM images (1 × 1 μm^2) of mixed C_8TAB−PSS LB films transferred at π = 10 mN/m onto mica. The surfactant/polymer ratios are 0.2 (a), 2.0 (b), and 5.0 (c).

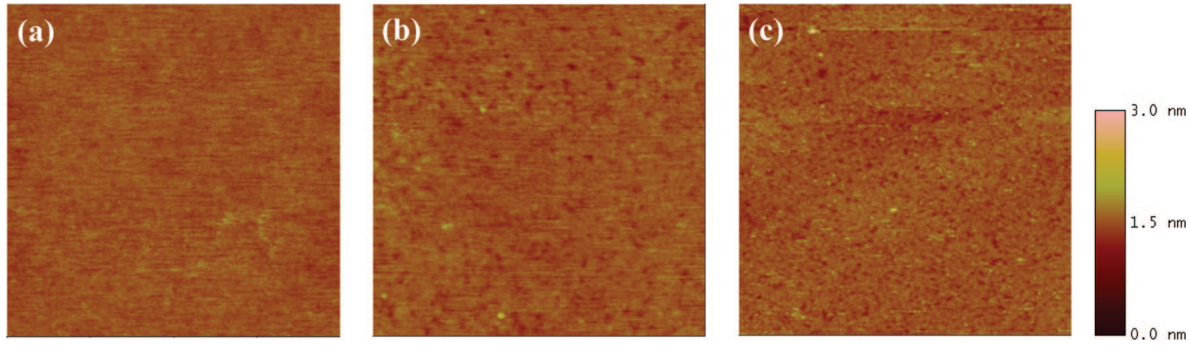

Figure 6. AFM images (1 × 1 μm^2) of mixed $C_{14}TAB$−PSS LB films transferred at π = 25 mN/m onto mica. The surfactant/polymer ratios are 0.2 (a), 1.0 (b), and 5.0 (c).

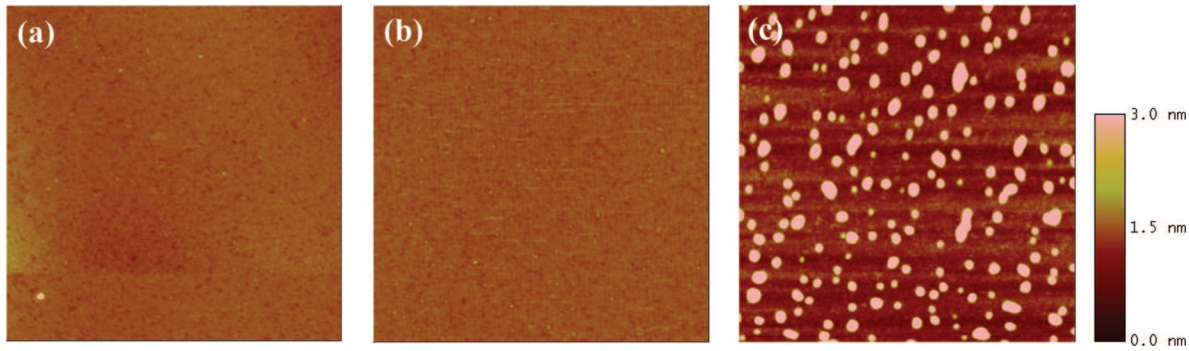

Figure 7. AFM images (1 × 1 μm^2) of mixed $C_{18}TAB$−PSS LB films transferred at π = 25 mN/m onto mica. The surfactant/polymer ratios are 0.2 (a), 1.0 (b), and 5.0 (c).

reasons leading to the appearance of holes in a monolayer include (1) the cohesive interaction between molecules is higher than the molecule−subphase interaction so that the monolayer cannot fully extend and (2) the molecule has a high solubility in water and the monolayer may be dissolved during compression. For the present case, it seems reasonable to attribute the morphology of $C_{14}TA$−PSS film to its higher solubility. However, the effect of the first term cannot be neglected completely. It is noteworthy that the incorporated ratio of surfactant to SPSS is about 1:1 for $C_{14}TA$−PSS and 0.9:1 for $C_{18}TA$−PSS, which also means that there are free PSS units in $C_{18}TA$−PSS but all the PSS units in $C_{14}TA$−PSS were paired by surfactant molecules. The residual PSS units in $C_{18}TA$−PSS monolayer should be negatively charged which contributes to the extension of the monolayer not only by increasing the monolayer−subphase interaction but also by preventing chain cohesion through Coulombic repulsion.

The AFM results shown above indicate that the main factor determining the film morphology of a mixed surfactant−PSS monolayer is the chain length of the incorporated surfactant. However, for the cospreading method, the slight variation of film morphology with the surfactant/PSS ratio indicates the various chain configurations of the mixed monolayers probably through the variation of monolayer composition. For more intensive study, the surface compositions of the mixed monolayers were determined by XPS analysis of the corresponding LB films, and the results are also shown in Table 1.

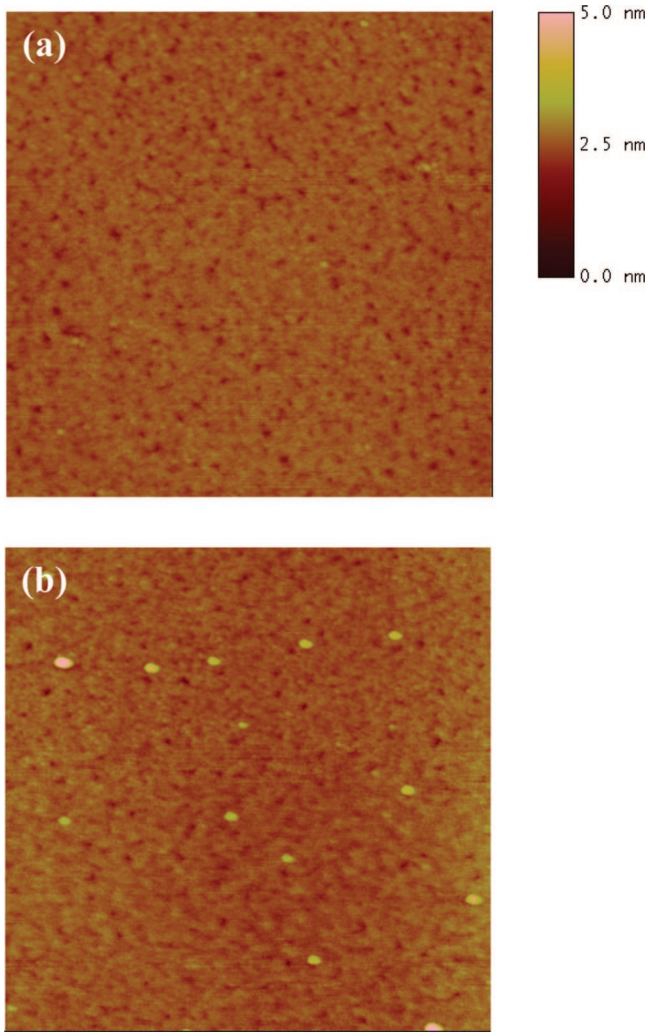

Figure 8. AFM images (1 × 1 μm^2) of mixed $C_{14}TA-PSS$ (a) and $C_{18}TA-PSS$ (b) complex monolayers prepared by preprecipitation.

It is interesting to find that, when the surfactant/polymer ratio in the spreading solvent is low (0.2), the N/S ratios measured from the LB films are as high as 1.67−1.86 for the three systems, which means that surfactant molecules existing at the air/water interface are about 1.7 times the value of PSS units. This result indicates that the $C_nTAB-PSS$ interaction does not only limit the electrostatic interaction between oppositely charged head groups but also involves other interactions such as VDW and polar−polar interactions. It is also possible that micelles and/or other aggregates of the surfactant can be formed around PSS cores, leading to a higher surfactant composition. However, since these aggregative structures are not detectable by AFM analysis, the probability of this process at low surfactant ratio (0.2) is very low.

When surfactant/polymer ratios corresponding to the rightmost shift of the isotherms were used (2.0 for $C_8TAB-PSS$ and 1.0 for the other two), the N/S ratio on the corresponding LB film is about 1.03 for $C_8TAB-PSS$ and about 0.9 for the other two systems. Under these conditions, the electrostatic interaction is supposed to be the major interaction for the complexes present at the air/water interface. Therefore, the N/S ratios tell that about a 1:1 incorporation ratio of C_8TAB-to-PSS unit is required for this complex to remain at the air/water interface. However, for $C_{14}TAB$ and $C_{18}TAB$, a smaller incorporated ratio is required.

With further increase of C_nTAB/PSS ratio to 5.0, the N/S ratio does not change significantly for the $C_8TAB-PSS$ system,

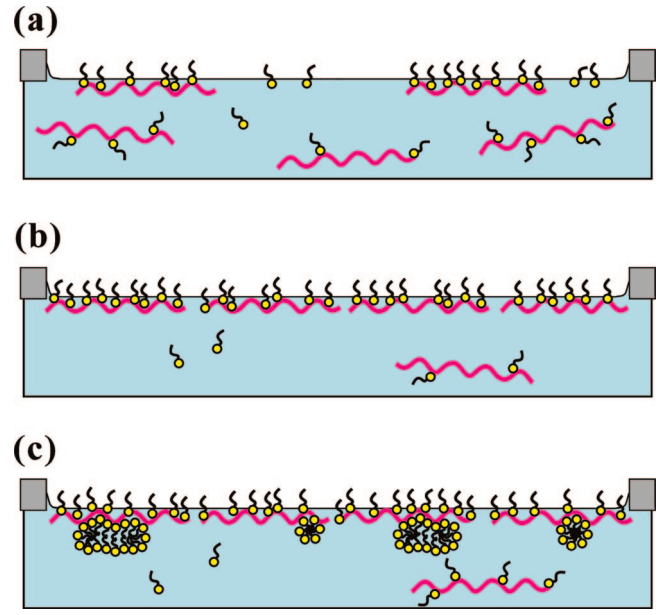

Figure 9. Proposed model illustrating the status of surfactant−polymer complexes and free surfactant molecules adsorbed at the air/water interface in the initial spreading stage for the cospreading approach. (A) Surfactant/polymer = 0.2: fewer complexes stably adsorb at the interface, and there are free areas on which the free surfactant can adsorb. (B) Surfactant/polymer = 1.0 or 2.0: most of the spread polymers present at the interface, and the free area for surfactant adsorption is low. (C). For the C18TAB−PSS at S/P = 5.0: the local surfactant concentration near the interface may reach a value high enough to cause micellization or aggregation around PSS cores.

which not only implies a weak VDW interaction in the $C_8TAB-PSS$ system but also confirms the low probability for surfactant aggregation around the complex. For $C_{14}TAB-PSS$ and $C_{18}TAB-PSS$ systems, the N/S ratio increases to 1.11 and 1.29, respectively, as C_nTAB/PSS ratio increases to 5.0. Apparently, the VDW and polar−polar interactions appear to be important for the systems using the longer surfactants. Since no observable aggregate was detected on the $C_{14}TAB-PSS$ LB film, the increase of N/S ratio is ascribed mainly to the presence of unbound surfactant. For the $C_{18}TAB-PSS$ system, however, both the unbound surfactant and the surfactant micellization around PSS cores should be responsible for its higher N/S ratio and the observed aggregates.

Proposed Model for the Incorporation of Surfactant and Polyelectrolyte at the Air/Water Interface. On the basis of the behavior of the mixed monolayers mentioned above, a model was proposed to depict the incorporation and spreading of the surfactant−polyelectrolyte complexes at the air/water interface for the cospreading method. It is inferred that the $C_nTAB-PSS$ interaction can occur in the spreading solvent or at the spreading stage on the subphase. For the complexes, only those with sufficient hydrophobicity can stay at the water surface, while the others should disperse into the subphase. In addition to the complex, some surfactant molecules, due to their amphiphilic characteristic, are also able to stay on the subphase, but the amount is determined by the free area available for adsorption and the adsorption free energy of a surfactant. Figure 9 shows a proposed model illustrating the status of the mixed monolayer before compression. In the following compression process, some of the surfactant molecules desorb out of the interface (especially for the C_8TAB), but some incorporate with neighboring complexes due to VDW and/or polar interaction.

When the C_nTAB/PSS ratio is low (0.2) in the spreading solvent (Figure 9a), there are fewer surfactant molecules for association with the PSS; therefore, fewer $C_nTAB-PSS$ com-

plexes are hydrophobic enough to be present at the air/water interface, and a large fraction of the spread PSS exists in the bulk water in either uncomplexed or complexed form. In such a case, there are more free areas at the interface on which the free surfactant can adsorb. The adsorbed surfactant molecules may be comparable to the C_nTAB−PSS complexes at the interface. Therefore, N/S ratios as high as 1.7 were obtained on the corresponding LB films. With increasing C_nTAB/PSS ratio in the spreading solvent (Figure 9b), more C_nTAB−PSS complexes are able to stay at the interface. The increase of complexed molecules at the interface results in a right shift of the isotherms; furthermore, the free area for surfactant adsorption decreases simultaneously. Therefore, the N/S ratio in the LB films decreases because fewer surfactant molecules were present in comparison with the system with a low C_nTAB/PSS ratio.

When the right-most shift state of the isotherm was approached, the amount of the stable complexes present at the interface attains an approximately constant value, which also means that the available surface area for surfactant adsorption does not vary significantly with further increase in the C_nTAB/PSS ratio. For the C_8TAB−PSS system, the N/S value for the LB film prepared at C_8TAB/PSS = 2.0 is 1.03 and at C_8TAB/PSS = 5.0 is 1.07. The nearly identical N/S value for the two conditions indicates that the high excess amount of surfactant added in the spreading solvent has little effect on increasing the concentration of adsorbed C_8TAB, attributable to the low hydrophobicity of C_8TAB. However, for the C_{14}TAB−PSS and C_{18}TAB−PSS systems, a further increase of N/S value was observed when the C_nTAB/PSS ratio was increased from 1.0 to 5.0. For the C_{14}TAB−PSS, the further incorporation of surfactant to the interface should be due to the unbound surfactant without forming an observable aggregative structure (as confirmed by the AFM image). For the C_{18}TAB−PSS system, the high surfactant concentration induces micellization of C_{18}TAB around PSS core, forming apparent aggregates shown in Figure 7c. The situation is schematically illustrated in Figure 9c. This mechanism causes not only a higher composition of surfactant in the LB film (N/S = 1.29) but also a further right shift of the isotherm.

Conclusion

On the basis of this study, a stable Langmuir monolayer of polyelectrolyte−surfactant complex can be prepared by cospreading a mixed solution at the air/water interface. The characteristics of a cospread monolayer are similar to the complex monolayers of the corresponding systems prepared by preprecipitation of the complexes from an aqueous solution. The complex monolayer prepared by incorporation using a longer chain surfactant has a higher collapse pressure, better relaxation stability, and a more condensed morphology. The XPS analysis indicates that surfactant molecules may be present in the monolayer as complexed or uncomplexed molecules. For the mixed monolayer prepared at low surfactant/polymer (S/P) ratio, fewer complexes have the ability to stably stay at the air/water interface and the uncomplexed surfactant may adsorb on the free area, leading to a higher surfactant composition relative to the monomer units of polyelectrolyte. With increasing S/P ratio, more stable complexes form at the interface which also decreases the adsorbed molecules of uncomplexed surfactant. The formation of the maximum amount of complexes are approached at S/P ratio of 1.0 or 2.0, where the composition of the uncomplexed surfactant is insignificant. A further increase of S/P ratio may cause an additional incorporation of uncomplexed surfactant (for C_{14}TAB−PSS) or micellization of surfactant around PSS cores (for C_{18}TAB−PSS).

Acknowledgment. The support of this research by the National Science Council of Taiwan through Grant NSC 96-2221-E-006-058 is gratefully acknowledged.

References and Notes

(1) Suzuki, M. *Thin Solid Films* **1989**, *180*, 253–261.
(2) Nishikata, Y.; Fukui, S.-I.; Kakimoto, M.-A.; Imai, Y.; Nishiyama, K.; Fujihira, M. *Thin Solid Films* **1992**, *210−211*, 296–298.
(3) Nishikata, Y.; Suwa, T.; Kakimoto, M.-A.; Imai, Y. *Thin Solid Films* **1992**, *210−211*, 390–392.
(4) Luzinov, I.; Minko, S.; Tsukruk, V. V. *Prog. Polym. Sci.* **2004**, *29*, 635–698.
(5) Li, Y.; Yang, M. J.; She, Y. *Talanta* **2004**, *62*, 707–712.
(6) Wagner, J.; Michel, T.; Nitsch, W. *Langmuir* **1996**, *12*, 2807–2812.
(7) Dobrynin, A. V.; Rubinstein, M. *Prog. Polym. Sci.* **2005**, *30*, 1049–1118.
(8) Hayakawa, K.; Kwak, J. C. T. *J. Phys. Chem.* **1982**, *86*, 3866–3870.
(9) Hayakawa, K.; Kwak, J. C. T. *J. Phys. Chem.* **1983**, *87*, 506–509.
(10) Asnacios, A.; Langevin, D.; Argillier, J. F. *Macromolecules* **1996**, *29*, 7412–7417.
(11) Asnacios, A.; Klitzing, R.; Langevin, D. *Colloids Surf., A* **2000**, *167*, 189–197.
(12) Monteux, C.; Williams, C. E.; Meunier, J.; Anthony, O.; Bergeron, V. *Langmuir* **2004**, *20*, 57–63.
(13) Monteux, C.; Llauro, M.-F.; Baigl, D.; Williams, C. E.; Anthony, O.; Bergeron, V. *Langmuir* **2004**, *20*, 5358–5366.
(14) Monteux, C.; Williams, C. E.; Bergeron, V. *Langmuir* **2004**, *20*, 5367–5374.
(15) Noskov, B. A.; Loglio, G.; Miller, R. *J. Phys. Chem. B* **2004**, *108*, 18615–18622.
(16) Noskov, B. A.; Loglio, G.; Lin, S. Y.; Miller, R. *J. Colloid Interface Sci.* **2006**, *301*, 386–394.
(17) Puggelli, M.; Gabrielli, G. *Colloid Polym. Sci.* **1983**, *261*, 667–671.
(18) Chi, L. F.; Johnston, R. R.; Ringsdorf, H. *Langmuir* **1991**, *7*, 2323–2329.
(19) Thalberg, K.; van Stam, J.; Lindblad, C.; Almgren, M.; Lindman, B. *J. Phys. Chem.* **1991**, *95*, 8975–8982.
(20) Michel, T.; Nitsch, W. *Thin Solid Films* **1994**, *242*, 234–238.
(21) Bergeron, V.; Langevin, D.; Asnacios, A. *Langmuir* **1996**, *12*, 1550–1556.
(22) Deo, P.; Deo, N.; Somasundaran, P.; Moscatelli, A.; Jockusch, S.; Turro, N. J.; Ananthapadmanabhan, K. P.; Ottaviani, M. F. *Langmuir* **2007**, *23*, 5906–5913.
(23) Taylor, D. J. F.; Thomas, R. K.; Penfold, J. *Adv. Colloid Interface Sci.* **2007**, *132*, 69–110.
(24) Thalberg, K.; Lindman, B.; Karlström, G. *J. Phys. Chem.* **1991**, *95*, 3370–3376.
(25) Almgren, M.; Jansson, P.; Muchtar, E.; van Stam, J. *Langmuir* **1992**, *8*, 2405–2412.
(26) Hansson, P.; Almgren, M. *Langmuir* **1994**, *10*, 2115–2124.
(27) Davis, F.; Hodge, P.; Liu, X.-H.; Ali-Adib, Z. *Macromolecules* **1994**, *27*, 1957–1963.
(28) Salfer, R.; Michel, T.; Nitsch, W. *Colloids Surf., A* **2002**, *210*, 253–264.
(29) Lee, W.; Ni, S.; Deng, J.; Kim, B.-S.; Satija, S. K.; Mather, P. T.; Esker, A. R. *Macromolecules* **2007**, *40*, 682–688.
(30) Jain, N. J.; Albouy, P.-A.; Langevin, D. *Langmuir* **2003**, *19*, 8371–8379.
(31) Jain, N. J.; Albouy, P.-A.; Langevin, D. *Langmuir* **2003**, *19*, 5680–5690.
(32) Rao, A.; Kim, J.; Thomas, R. R. *Langmuir* **2005**, *21*, 617–621.
(33) Rao, A.; Kim, Y.; Kausch, C. M.; Thomas, R. R. *Langmuir* **2006**, *22*, 7964–7968.
(34) Griffiths, P. C.; Roe, J. A.; Bales, B. L.; Pitt, A. R.; Howe, A. M. *Langmuir* **2000**, *16*, 8248–8254.
(35) Taylor, D. J. F.; Thomas, R. K.; Li, P. X. *Langmuir* **2003**, *19*, 3712–3719.

MA800855H